American Mineralogist, Volume 90, pages 411–416, 2005

The crystal structures of synthetics $Fe_2(SO_4)_3(H_2O)_5$ and the type specimen of lausenite

Juraj Majzlan,[1,*] Cristian Botez,[2,3] and Peter W. Stephens[2,3]

[1]Department of Geosciences, Princeton University, Princeton, New Jersey 08544, U.S.A.
[2]Department of Physics and Astronomy, State University of New York, Stony Brook, New York 11794, U.S.A.
[3]National Synchrotron Light Source, Brookhaven National Laboratory, Upton, New York 11973, U.S.A.

Abstract

An iron sulfate of nominal composition $Fe_2(SO_4)_3(H_2O)_5$ has been synthesized and its structure determined and refined by high resolution powder diffraction using synchrotron radiation. The structure consists of corrugated slabs in which iron octahedra are linked by sulfate tetrahedra in the monoclinic space group $P2_1/m$ with lattice parameters a = 10.711(1), b = 11.085(1), and c = 5.5747(5) Å, β = 98.853(3)°. We compare these results with the type specimen of lausenite from Jerome, Arizona, which has monoclinic lattice parameters a = 10.679(2), b = 11.053(3), and c = 5.567(1) Å, β = 98.89(1)°. Weight loss experiments show that it is currently a pentahydrate, despite earlier reports that lausenite is a hexahydrate. We argue that our synthetic material provides a structure determination for the type specimen of lausenite.

Introduction

Iron sulfate minerals are common and locally abundant products of weathering of pyrite and occasionally other sulfide minerals. They are distinct markers of acid mine drainage (AMD) pollution (e.g., Ash et al. 1951; Nordstrom et al. 2000; Buckby et al. 2003). These minerals are able to store and release toxic metals and acidity, and therefore are of interest with respect to remediation activities at AMD sites. Many of the AMD minerals belong to the Fe_2O_3-SO_3-H_2O system which was systematically studied by Posnjak and Merwin (1922) and Merwin and Posnjak (1937). The crystal structures of most of the Fe_2O_3-SO_3-H_2O phases are known from single-crystal studies of natural specimens. One remaining mineral in this system is lausenite, a rare and poorly characterized phase. The structure and most physical properties of lausenite are unknown.

Using the phase diagram of Posnjak and Merwin (1922), we synthesized a phase corresponding to their $Fe_2(SO_4)_3(H_2O)_6$ compound and investigated its spectroscopic and thermodynamic properties. The results of these investigations will be reported elsewhere. Interpretation of these results and their placement into the context of the studied chemical system is predicated upon knowledge of its composition and structure. Because only fine-grained powders could be synthesized, the structure was solved from powder X-ray diffraction data. Having solved the structure of this synthetic phase, we investigated the relationship between this structure and the structure of the mineral lausenite.

Experimental methods

$Fe_2(SO_4)_3(H_2O)_5$ was synthesized from a mixture of deionized water, sulfuric acid (96 wt% H_2SO_4, ρ = 1.84 g/cm^3, reagent grade, Fisher) and fine-grained, homogeneous hydrated ferric sulfate [$Fe_2(SO_4)_3(H_2O)_x$, reagent grade, Alfa Aesar]. The amount of water, x, in the ferric sulfate reagent, was determined to be ~6.75 by a thermogravimetric analysis. The solution from which $Fe_2(SO_4)_3(H_2O)_5$ precipitated was prepared by mixing 1.52 mL water, 0.48 mL sulfuric acid, and 1.98 g of ferric sulfate. The solution was then kept at 90 °C for a week. A pale pink product was separated from the mother liquor by filtration, washed with copious amounts of anhydrous methanol, and dried at room temperature.

The type specimen of lausenite from Jerome, Arizona, collected by Lausen in the 1920s and deposited with the Harvard Mineralogical Museum (HMM no. 90537), was kindly made available to us. The sample has been kept in a wax-sealed vial, and showed no signs of decomposition, such as growth of new phases on the surface of the sample, evidence of deliquescence, etc.

Preliminary X-ray diffraction (XRD) experiments were carried out with a Bragg-Brentano geometry Scintag PAD V diffractometer in flat-plate geometry, with Cu$K\alpha$ radiation, and a diffracted-beam graphite monochromator. These experiments confirmed that the XRD pattern of the synthesized phase does not match those Fe_2O_3-SO_3-H_2O phases whose structures are known. This diffractometer was also used to collect an XRD pattern from the natural lausenite sample.

Thermogravimetric (TG) and differential thermal (DT) analysis was performed with a Netzsch 449 instrument. The sample was loaded into a Pt crucible, covered with a Pt lid, and heated from 25 to 800 °C at a rate of 10 °C/min with a continuous oxygen flow of 40 mL/min. An experiment with empty crucibles was performed to correct for the buoyancy of the gas. Simultaneously with the thermal analysis experiment, the evolved gases were fed into a Bruker Equinox 55 Fourier-transform infrared (FTIR) spectrometer. The signal in the energy range of 1000–4000 cm^{-1} was collected with a liquid nitrogen cooled MCT detector.

Weight loss upon firing was measured by heating a known amount of the sample in corundum crucibles at 950 °C overnight. Prior to the measurements, the corundum crucibles were repeatedly annealed at 1500 °C overnight until no weight change could be recorded. The crucibles with sample were weighed before and after heating with a balance with a manufacturer-stated precision of 0.01 mg.

The XRD pattern for structure solution was collected at the bending magnet beamline X3B1 at the National Synchrotron Light Source (Brookhaven National Laboratory). X-rays of wavelength of 1.14959(1) Å were selected by a double crystal Si(111) monochromator. The wavelength and the zero angle of the diffractometer were determined with a NIST 1976 standard reference material (corundum, α-Al_2O_3). The sample was loaded into a 1.0 mm glass capillary which was rotated about its axis during the data collection. The intensity of the incoming beam was monitored during the data collection with an ion chamber and the measured intensities of the diffracted beam were corrected for the decay and fluctuations of the primary beam. The diffracted beam was analyzed with a Ge(111) crystal and a Na(Tl)I scintillation detector. The XRD pattern was collected at room temperature, over an angular range of 5.9 to 65.9° 2Θ, with a step size of 0.003°, and counting time of 2 s per point.

* E-mail: Juraj.Majzlan@minpet.uni-freiburg. Present Address: Institute of Mineralogy, Petrology and Geochemistry, Albert-Ludwig-University of Freiburg, Albertstr. 23b, Freiburg, D-79104, Germany.

0003-004X/05/0203–411$05.00/DOI: 10.2138/am.2005.1701

Results

Thermal analysis

The DT and TG traces of the synthetic sample (Fig. 1) show two endothermic weight loss events. The first one, at ~250 °C, corresponds to an H_2O weight loss of 18.0%. The second event at 690 °C is typical of decomposition of anhydrous $Fe_2(SO_4)_3$ to hematite (α-Fe_2O_3) and the evolution of sulfur oxide gases. The TG results suggest that the sample contains ~33% Fe_2O_3, and, by difference, ~49% SO_3. The weight per cent ratio of Fe_2O_3 and SO_3 corresponds to a molar ratio of Fe:S = 2:3. A more precise determination of the Fe_2O_3 content of the sample was obtained by comparing its weight before and after heating to 950 °C. Six such measurements gave an average of 32.56(10) wt% Fe_2O_3, which leads to a formula of $Fe_2(SO_4)_3(H_2O)_{5.02}$ for our sample.

Structure solution and description

Using the synchrotron data, twenty-five low angle peaks were used for initial unit cell indexing with ITO (Visser 1969). A monoclinic solution with $a = 10.711$, $b = 11.084$, and $c = 5.574$ Å, and $\beta = 98.85°$, and a figure of merit of 341 was accepted for further work. Systematic extinctions suggested possible space groups $P2_1$ or $P2_1/m$. In the case of space group $P2_1$, the density and unit cell volume implies that there should be one formula unit in the irreducible cell with all atoms located at general positions. Space group $P2_1/m$ would require substantially fewer atoms at general positions, and some of the atoms would have to be located on the mirror plane.

We sought to solve the structure using the direct methods program for powder data, EXPO (Altomare et al. 1999), for both space groups. EXPO extracted the integrated intensities and found a candidate solution in space group $P2_1$ with 22 atoms in the asymmetric cell and a candidate solution in space group $P2_1/m$ with 14 atoms in the asymmetric cell. Initially, the $P2_1$ model was transferred to the Rietveld refinement program GSAS (Larson and Von Dreele 1994). Peak profile parameters of the pseudovoigt function and the diffractometer zero were refined in the early stages and later kept constant. Rigid bodies were inserted at the positions of the sulfate tetrahedra, and the parameters describing the rigid bodies were refined. Subsequently, the rigid bodies were removed, and the positions of all the atoms were refined with significant damping on the shift of atomic coordinates. Rigid bodies were placed at the positions of the Fe octahedra, refined, removed, and the positions of all of the atoms were again refined independently. The damping was removed, and soft restraints were imposed on the S-O bond lengths and O-S-O and O-Fe-O bond angles. These restraints were not removed throughout the final stages of refinement. The distance and angle restraints contributed 0.7 and 5.8%, respectively, to the total χ^2. Isotropic thermal factors were constrained to be identical for all atoms of the same element. An absorption correction was modeled using the Hewat function in GSAS, with absorption coefficient fixed at a value derived from chemical composition, calculated density of the sample, and an assumed 50% packing fraction. The lattice parameters, molar volume, calculated density, and statistics of the refinement are given in Table 1. The final values of atomic positions and displacement parameters are listed in Table 2. The pattern calculated from the refined parameters compares well to the experimental XRD pattern (Fig. 2). Bond lengths and angles are listed in Table 3. The XRD pattern, (d spacings, relative intensities, indices), is tabulated in a standard format.[1]

The $P2_1/m$ model was also refined in GSAS, with the approximate starting positions of the atoms derived from the $P2_1$ model. The statistical parameters for both models were similar. We gave preference to be $P2_1/m$ model because, in addition to being simpler, it seemed to converge faster and be more stable at the refinement minimum.

There are several small peaks (d = 3.957, 3.043, 2.731, 2.605, 2.581, 2.434, 2.275, 2.006 Å) in the synchrotron XRD pattern that remain unindexed. We were not able to assign these peaks to a specific phase or phases. The stability field of the studied phase is flanked by $Fe(OH)(SO_4)$, kornelite [$Fe_2(SO_4)_3(H_2O)_{7.25}$],

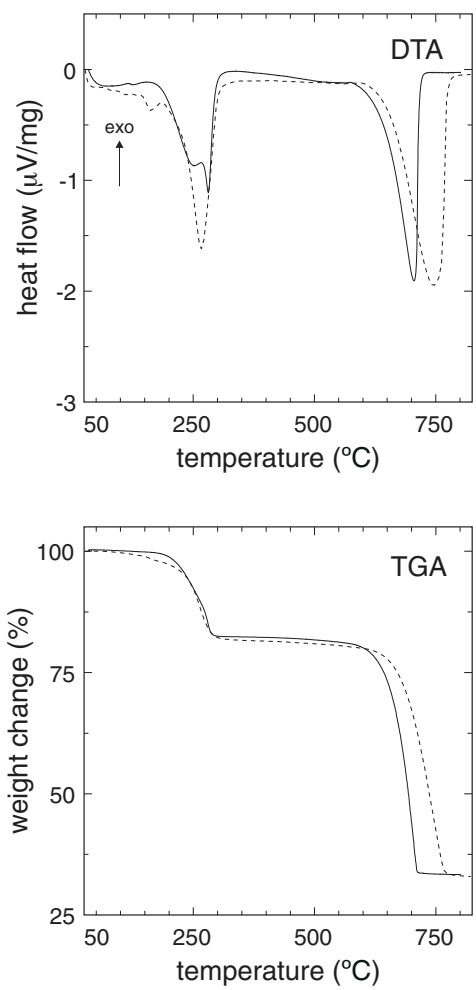

Figure 1. TGA and DTA traces of synthetic $Fe_2(SO_4)_3(H_2O)_5$ (solid curves) and the type specimen of lausenite (dashed curves).

[1]For a copy of the XRD pattern, document item AM-05-008, contact the Business Office of the Mineralogical Society of America (see inside front cover of recent issue) for price information. Deposit items are available on the American Mineralogist web site at http://www.minsocam.org (or contact MSA Business Office for updated link information).

and rhomboclase [$(H_3O)Fe^{3+}(SO_4)_2(H_2O)_3$] (Posnjak and Merwin 1922). However, the patterns of these phases did not match the observed impurity peaks.

The structure of $Fe_2(SO_4)_3(H_2O)_5$ contains two symmetrically distinct Fe^{3+} cations, each of which is octahedrally coordinated. Fe1 is coordinated by four bridging O atoms and two water molecules. Fe2 is coordinated by three bridging O atoms and three water molecules. In both cases, the bond distances to the water molecules are significantly longer than those to the bridging O atoms (Table 3). We were unable to locate the H atoms from the difference Fourier maps.

Two symmetrically distinct S^{6+} cations are tetrahedrally coordinated. S1 shares three bridging O atoms with the neighboring Fe octahedra, while S2 shares only two. The distances from sulfur ions to the bridging O atoms are slightly longer than those to the terminal O atoms (Table 3).

Iron octahedra are connected solely via sulfate tetrahedra, i.e., there are no bridging O atoms between two iron ions. The polyhedra connect to form corrugated slabs parallel to the **yz** plane (Fig. 3). Slabs composed of the same type of polyhedral units are found in the structure of kornelite, $Fe_2(SO_4)_3(H_2O)_{7.25}$ (Robinson and Fang 1973). The structures of the higher hy-

TABLE 1. Crystallographic data and the statistics of Rietveld refinement for $Fe_2(SO_4)_3(H_2O)_5$

Molecular weight	489.96 g/mol
Space group	$P2_1/m$
Z	2
Lattice parameters	a = 10.711(1) Å
	b = 11.085(1) Å
	c = 5.5747(5) Å
	β = 98.853(3)°
Cell volume	654.0(2) Å^3
Molar volume	196.9 cm^3/mol
Calculated density	2.49 g/cm^3
Number of data points	19999
Le Bail χ^2	4.07
Rietveld χ^2	4.05
Rietveld wR_p	14.7%

TABLE 2. Fractional atomic coordinates and isotropic displacement parameters (in Å^2) for $Fe_2(SO_4)_3(H_2O)_5$

Atom	x	y	z	U_{iso}	Wyckoff position
Fe1	1/2	1/2	1/2	0.0222(5)	2*d*
Fe2	0.1262(2)	3/4	0.8933(5)	0.0222(5)	2*e*
S1	0.4056(4)	3/4	0.2163(6)	0.0251(8)	2*e*
S2	0.2233(2)	0.0020(3)	0.6695(5)	0.0251(8)	4*f*
O1	0.4729(8)	3/4	0.006(1)	0.0457(9)	2*e*
O2	0.2689(6)	3/4	0.139(2)	0.0457(9)	2*e*
O3	0.3627(4)	0.4928(6)	0.705(1)	0.0457(9)	4*f*
O4	0.1902(5)	0.0657(5)	0.876(1)	0.0457(9)	4*f*
O5	0.1673(6)	0.0399(5)	0.430(1)	0.0457(9)	4*f*
O6	0.4277(6)	0.8529(3)	0.3713(8)	0.0457(9)	4*f*
O7	0.1855(6)	0.6238(4)	0.705(1)	0.0457(9)	4*f*
Ow1	0.3985(6)	0.4147(5)	0.209(1)	0.0457(9)	4*f*
Ow2	−0.0518(8)	3/4	0.686(2)	0.0457(9)	2*e*
Ow3	0.0536(6)	0.8728(5)	0.112(1)	0.0457(9)	4*f*

Note: Numbers in parentheses are the statistical estimated standard deviations of the last digit from the Rietveld refinement, and are substantially smaller than any realistic estimate of accuracy.

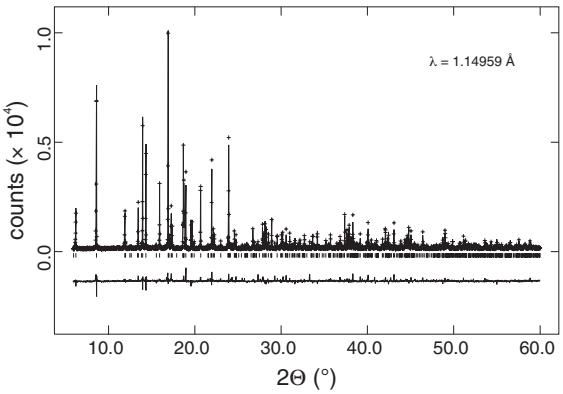

FIGURE 2. Synchrotron X-ray diffraction pattern of $Fe_2(SO_4)_3(H_2O)_5$ with the calculated and difference plot from the Rietveld refinement.

TABLE 3. Bond lengths (Å) and angles (°) in the structure of $Fe_2(SO_4)_3(H_2O)_5$

Fe1-O3 (×2)	2.00(1)	S1-O1	1.47(1)
Fe1-O6 (×2)	1.90(1)	S1-O2	1.46(1)
Fe1-Ow1 (×2)	2.04(1)	S1-O6 (×2)	1.43(1)
Fe2-O2	1.89(1)	S2-O3	1.48(1)
Fe2-O7 (×2)	1.92(1)	S2-O4	1.44(1)
Fe2-Ow2	2.07(1)	S2-O5	1.44(1)
Fe2-Ow3 (×2)	2.06(1)	S2-O7	1.47(1)
Ow1-Fe1-O3	95.0(1)	Ow2-Fe2-Ow3	86.1(1)
Ow1-Fe1-O3	85.0(1)	Ow2-Fe2-O7	92.8(1)
Ow1-Fe1-O6	92.2(1)	O2-Fe2-Ow3	84.7(1)
Ow1-Fe1-O6	87.8(1)	O2-Fe2-O7	95.6(1)
O3-Fe1-O6	92.5(1)	Ow3-Fe2-Ow3	82.9(1)
O3-Fe1-O6	87.5(1)	Ow3-Fe2-O7	91.6(1)
		O7-Fe2-O7	93.8(1)
O3-S2-O4	104.1(1)		
O3-S2-O5	112.3(1)	O1-S1-O2	111.0(1)
O3-S2-O7	108.1(1)	O1-S1-O6	115.3(1)
O4-S2-O5	118.7(1)	O2-S1-O6	104.1(1)
O4-S2-O7	104.5(1)	O6-S1-O6	106.0(1)
O5-S2-O7	108.5(1)		

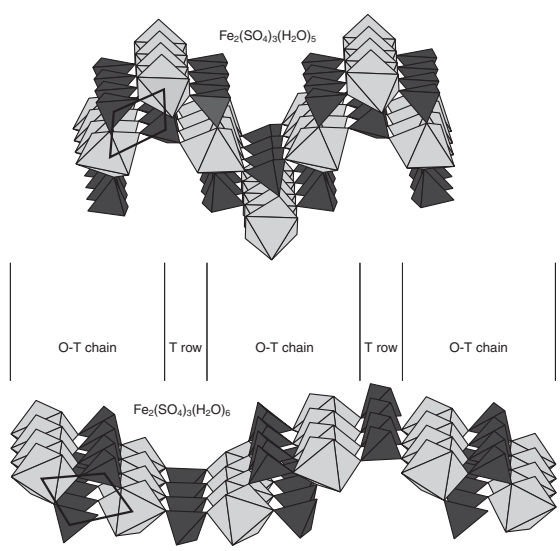

FIGURE 3. Polyhedral representation of the corrugated $Fe_2(SO_4)_3(H_2O)_5$ slabs which build the structure of this phase, and the $Fe_2(SO_4)_3(H_2O)_6$ slabs in the structure of kornelite. The octahedral-tetrahedral (O-T) chains and rows of sulfate tetrahedra are marked in the structure of kornelite. The O-T chains in both structures are highlighted by thick rhombohedral outlines.

drates coquimbite [$Fe_2(SO_4)_3(H_2O)_9$; Fang and Robinson 1970] and quenstedtite [$Fe_2(SO_4)_3(H_2O)_{11}$; Thomas et al. 1974] are depolymerized, composed of isolated clusters.

The structure of $Fe_2(SO_4)_3(H_2O)_5$ is similar, but not identical, to the crystal structures of $Al_2(SO_4)_3(H_2O)_5$ (Fischer et al. 1996) and $In_2(SeO_4)_3(H_2O)_5$ (Kadoshnikova et al. 1978). The small differences among these structures are depicted in Figure 4.

Discussion

The phase whose structure is reported here is a pentahydrate of $Fe_2(SO_4)_3$. On the other hand, Posnjak and Merwin (1922) reported only the existence of anhydrous Fe^{3+} sulfate, its hexahydrate, and heptahydrate. In addition, nonahydrate and undecahydrate are also known as the minerals coquimbite and quenstedtite, respectively. The phase reported by Posnjak and Merwin (1922) as $Fe_2(SO_4)_3(H_2O)_6$ was synthesized at temperatures of 50–150 °C from solutions with identical composition as used in this work, and has physical properties very similar to the phase studied in this work. Likewise, the chemical composition of the mineral lausenite was originally given as $Fe_2(SO_4)_3(H_2O)_6$ (Lausen 1928). Therefore, the relationship between the studied phase $Fe_2(SO_4)_3(H_2O)_5$ and lausenite must be clarified.

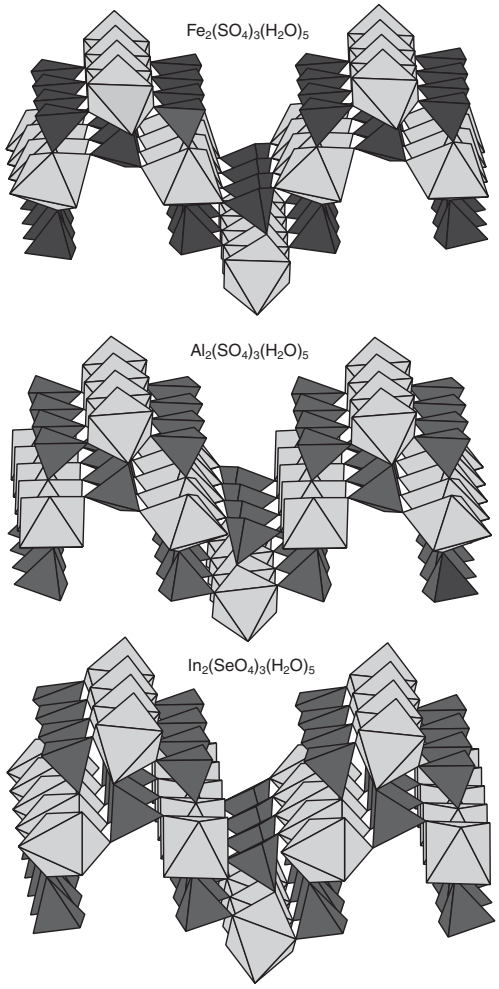

Figure 4. A comparison of the crystal structures of $Fe_2(SO_4)_3(H_2O)_5$, $Al_2(SO_4)_3(H_2O)_5$, and $In_2(SeO_4)_3(H_2O)_5$.

Natural occurrences of lausenite

Lausen (1928) investigated minerals that formed due to a long lasting fire in a pyrite mine near Jerome, Arizona, U.S.A. Among other minerals, he found one with approximate composition $Fe_{1.85}Al_{0.15}(SO_4)_3(H_2O)_6$ and associated this mineral with the phase described by Posnjak and Merwin (1922). Lausen (1928) proposed the name rogersite for the new mineral, but Butler (1928) pointed out that the name rogersite was already in use and suggested calling the mineral lausenite after its discoverer. Srebrodol'skiy (1975) described lausenite with composition $Fe_{1.03}Al_{1.00}(SO_4)_3(H_2O)_6$ from the burning dumps of the Velikomostovskaya coal mine in Ukraine. To our knowledge, no other reports of this mineral have been published.

A TG/DT analysis of the natural lausenite sample from Jerome, Arizona, shows an endothermic event at ~260 °C, accompanied by a weight loss of 18.3% (Fig. 1, Table 4). FTIR analysis of the evolved gases shows that only water is evolved in this step. In the second endothermic event, the weight loss of 47.2% corresponds to the evolution of SO_2, as documented by FTIR spectra of the liberated gases. The shift of the second endotherm to a higher temperature in comparison with synthetic $Fe_2(SO_4)_3(H_2O)_5$ (Fig. 1) is probably caused by the Al impurity in the natural sample. The values measured by TGA confirm that the stored lausenite specimen from Jerome, Arizona, is currently a pentahydrate of Fe^{3+} sulfate.

The powder X-ray diffraction pattern of the type specimen of

Table 4. Water content in the hydrates of Fe^{3+} sulfate

Sample	Wt% water
Synthetic sample (TGA)	18.0
Synthetic sample (firing experiments)	18.47
Natural sample, Jerome, Arizona (TGA)	18.3
$Fe_2(SO_4)_3(H_2O)_5$ (theoretical)	18.38
$Fe_2(SO_4)_3(H_2O)_6$ (theoretical)	21.28

Note: The method of determination is specified in parentheses. In the firing experiments, the measured quantity was wt% Fe_2O_3; water was calculated by difference, assuming a stoichiometric (1:3) ratio between Fe_2O_3 and SO_3.

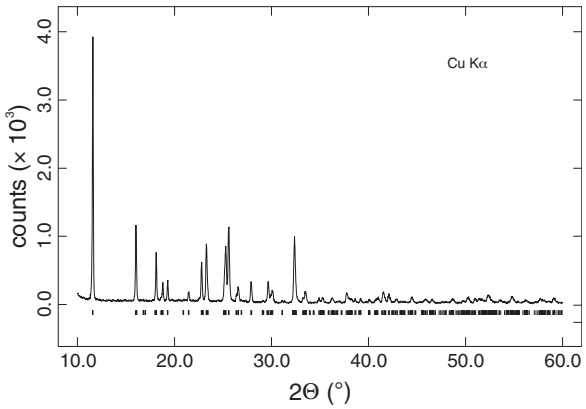

Figure 5. Powder X-ray diffraction pattern of lausenite with the calculated positions of the diffraction peaks. This pattern was collected in a flat-plate geometry, and the differences in relative intensities of the peaks in this pattern and the synchrotron pattern (cf. Fig. 2) is due to preferred orientation that could not be completely avoided in this geometry.

lausenite (Fig. 5, see also the Table in the MSA data depository) corresponds to the pattern of our synthesized sample. Using the structure of synthetic $Fe_2(SO_4)_3(H_2O)_5$ as the starting model, a profile fit of the XRD pattern of the natural sample gave lattice parameters a = 10.679(2), b = 11.053(3), and c = 5.567(1) Å, β = 98.89(1)°, V = 649.2(3) Å^3. The agreement between the starting structural model of $Fe_2(SO_4)_3(H_2O)_5$ and the profile fit for the natural sample confirms that the structures of these two samples are identical.

The only XRD data given by Srebrodol'skiy (1975) for his lausenite sample were a list of interplanar spacings and intensities for the strongest XRD peaks. Several of those peaks are not seen in either the synthetic sample or the type specimen of lausenite we studied. Srebrodol'skiy (1975) mentioned that the sample was contaminated with several other minerals, among them by a substantial amount of kieserite. The chemical analysis of this material also indicates that several phases must be present. The sample found by Srebrodol'skiy (1975) was probably a mixture of several phases, one of which may have been lausenite.

Lausenite: a hexahydrate or a pentahydrate?

There is a clear contradiction between the results of Posnjak and Merwin (1922), Lausen (1928), and Srebrodol'skiy (1975) on one hand, and our results on the other hand. A difference of 2.9 wt% of H_2O between a pentahydrate and hexahydrate of $Fe_2(SO_4)_3$ is certainly large enough to distinguish between the two hydration states. While the three earlier studies provide analyses which undoubtedly document the existence of hexahydrate, the same can be stated about our results with respect to the pentahydrate. The discrepancy can perhaps be resolved by inspecting the relationship between the structures of $Fe_2(SO_4)_3(H_2O)_5$ and kornelite ($Fe_2(SO_4)_3(H_2O)_{7.25}$) and their possible hydration states.

Kornelite is an intermediate hydrate in the family of hydrated $Fe_2(SO_4)_3$ phases. Its hydration state is tricky to ascertain because it is "difficult to free the crystals from the mother liquid without some decomposition" (Posnjak and Merwin 1922). They proposed that the phase is a heptahydrate. Robinson and Fang (1973) determined the crystal structure of kornelite and found that there are 7.25 H_2O molecules per $Fe_2(SO_4)_3$. The structure of kornelite is composed of slabs with composition $Fe_2(SO_4)_3(H_2O)_6$ (Fig. 3). The excess molecular water is located at partially occupied sites between these slabs (Robinson and Fang 1973). If the sites were fully occupied, the phase would be an octahydrate; when empty, the phase would be a hexahydrate. Robinson and Fang (1973) hypothesized that lausenite has the structure of kornelite with missing molecular water between the slabs. In other words, the kornelite structure could have a continuum of hydration states from hexahydrate to octahydrate, and lausenite would be the dehydrated end-member.

The slabs in the structure of kornelite can be constructed from spiral chains of iron octahedra and sulfate tetrahedra (O-T chains), linked by rows of sulfate tetrahedra (Fig. 3). The same structural units build the slabs in the studied $Fe_2(SO_4)_3(H_2O)_5$, only in a different arrangement. The transition from the kornelite-like slab to a slab in $Fe_2(SO_4)_3(H_2O)_5$ involves tilting of the O-T chains, liberation of one H_2O molecule and the formation of new bonds to the bridging O atoms coordinating the S^{6+} and Fe^{3+} ions. The rate of this transition will be dictated by the interplay of the requirement of slight reorganization of the structure and the necessity of breaking and forming bonds. The two structures may be intergrown, giving the Fe^{3+} sulfate further freedom of variable hydration states.

The structural similarity between kornelite and $Fe_2(SO_4)_3(H_2O)_5$ indicates that the hexahydrate may easily transform to a pentahydrate, if exposed to elevated temperatures, dehydrating agents, or low humidity. Drying the sample by anhydrous methanol, as done in this study, may be one of the possibilities for dehydration. We synthesized another batch of the sample but did not dry it with methanol. XRD patterns of the wet paste and unwashed filtrate showed that these are mixtures of $Fe_2(SO_4)_3(H_2O)_5$ and kornelite, with the latter predominant. No other phase could be detected from these patterns. Determination of water content in these samples is complicated because the solution cannot be completely removed without thorough washing. The type specimen, deposited in the Harvard Mineralogical Museum for almost 80 years, may also have dehydrated. The sample shows no obvious evidence of water loss, such as development of cracks. On the other hand, slow re-equilibration over the decades may have left the external shape of the sample unmodified. Whether any alteration took place remains unclear.

A direct comparison between the phases available to Posnjak and Merwin (1922) and Lausen (1928) is impossible, because neither reported an XRD pattern. Posnjak and Merwin (1922) did report precise data on refraction indices for most phases they studied. Their results can be compared to the mean refraction index (Table 5) calculated for each phase from the Gladstone-Dale relationship (Mandarino 1976). There is a good agreement for all phases. The refraction indices reported by Posnjak and Merwin (1922) and Lausen (1928) for their $Fe_2(SO_4)_3(H_2O)_6$ correspond very well to the calculated index for our $Fe_2(SO_4)_3(H_2O)_5$, suggesting that they may have studied the pentahydrate. It is possible that Posnjak and Merwin (1922) investigated both pentahydrate and hexahydrate. They provided only a single analysis of the solid, not specifying from which experiment this solid originated. Both increasing temperature and increasing molality of sulfuric acid can cause a transition from the stability of field of the hexahydrate to that of the pentahydrate. If the phases are very similar in their optical properties, the transition may go unnoticed.

In conclusion, the type specimen of lausenite is identical with

TABLE 5. Measured and calculated mean refraction indices for ferric sulfates

Phase	n_{meas}	n_{calc}
Kornelite	1.5993*	1.5995
$Fe_2(SO_4)_3(H_2O)_6$	1.6323*	
Lausenite	1.6267†	
$Fe_2(SO_4)_3(H_2O)_5$		1.6298
H_3O jarosite	1.7867*	1.8323
Mikasaite	1.7667*	1.7750
Butlerite	1.6717*	1.6827
Copiapite	1.5580*	1.5759
$Fe(OH)(SO_4)$	1.8353*	1.8204
Rhomboclase	1.5727*	1.5682

Notes: Measured data are a mean (see Mandarino 1976) of the refraction indices determined experimentally. Calculated data are derived from the Gladstone-Dale relationship, using densities calculated from structural data and the parameters given by Mandarino (1976).
* Posnjak and Merwin (1922).
† Lausen (1928).

the $Fe_2(SO_4)_3(H_2O)_5$ phase synthesized and studied in this work. Whether this lausenite sample has changed since Lausen's work in the 1920s remains unknown. The problem can be solved either by a new find of lausenite in nature, or by a detailed re-evaluation of the phase relationships in the system Fe_2O_3-SO_3-H_2O in the range of 50–150 °C.

Acknowledgments

We thank S. Krivovichev and R. Peterson for helpful comments that improved the manuscript, and C. Francis (Harvard Mineralogical Museum) for making available the type lausenite specimen. We are grateful to P. Burns for editorial handling of the manuscript and S. Ushakov for the help with the TGA/DTA/FTIR analysis of the lausenite specimen. J.M. appreciates the support that came with a Hess post-doctoral fellowship at the Department of Geosciences at Princeton University. This research was carried out in part at the National Synchrotron Light Source at Brookhaven National Laboratory, which is supported by the U.S. Department of Energy, Divisions of Materials Sciences and Chemical Sciences. The SUNY X3 beamline at NSLS was previously supported by the Division of Basic Energy Sciences of the U.S. Department of Energy under Grant No. DE-FG02-86ER45231.

References cited

Altomare, A., Burla, M.C., Camalli, M., Carrozzini, B., Cascarano, G., Giacovazzo, C., Guagliardi, A., Moliterni, A.G.G., Polidori, G., and Rizzi, R. (1999) EXPO: a program for full powder decomposition and crystal structure solution. Journal of Applied Crystallography, 32, 339–340.

Ash, S.H., Felegy, E.W., Kennedy, D.O., and Miller, P.S. (1951) Acid mine drainage problems—Anthracite region of Pennsylvania. U.S. Bureau of Mines Bulletin, 508.

Buckby, T., Black, S., Coleman, M.L., and Hodson, M.E. (2003) Fe-sulphate-rich evaporative mineral precipitates from the Rio Tinto, southwest Spain. Mineralogical Magazine, 67, 263–278.

Butler, G.M. (1928) In Corrections to volume 13. American Mineralogist, 13, 594.

Fang, J.H. and Robinson, P.D. (1970) Crystal structures and mineral chemistry of hydrated ferric sulfates. I. The crystal structure of coquimbite. American Mineralogist, 55, 1534–1540.

Fischer, T., Eisenmann, B., and Kniep, R. (1996) Crystal structure of dialuminium tris(sulfate) pentahydrate, $Al_2(SO_4)_3{\cdot}5H_2O$. Zeitschrift für Kristallographie, 211, 471–472.

Kadoshnikova, N.V., Shumyatskaya, N.G., and Tananaev, I.V. (1978) Synthesis and crystallographic structure of $In_2(SeO_4)_3{\cdot}5H_2O$. Doklady Akademii Nauk SSSR, 243, 116–118.

Larson, A.C. and von Dreele, R.B. (1994) GSAS. General Structure Analysis System. LANSCE, MS-H805, Los Alamos, New Mexico.

Lausen, C. (1928) Hydrous sulphates formed under fumerolic conditions at the United Verde mine. American Mineralogist, 13, 203–229.

Mandarino, J.A. (1976) The Gladstone-Dale relationship - Part I: Derivation of new constants. The Canadian Mineralogist, 14, 498–502.

Merwin, H.E. and Posnjak, E. (1937) Sulphate incrustations in the Copper Queen Mine, Bisbee, Arizona. American Mineralogist, 22, 567–571.

Nordstrom, D.K., Alpers, C.N., Ptacek, C.J., and Blowes, D.W. (2000) Negative pH and extremely acidic mine waters from Iron Mountain, California. Environmental Science and Technology, 34, 254–258.

Posnjak, E. and Merwin, H.E. (1922) The system, Fe_2O_3-SO_3-H_2O. Journal of the American Chemical Society, 44, 1965–1994.

Robinson, P.D. and Fang, J.H. (1973) Crystal structures and mineral chemistry of hydrated ferric sulphates. III. The crystal structure of kornelite. American Mineralogist, 58, 535–539.

Srebrodol'skiy, B.I. (1975) Lausenite, first find in the USSR. Doklady Akademii Nauk SSSR (Mineralogy), 219, 125–126.

Thomas, J.N., Robinson, P.D., and Fang, J.H. (1974) Crystal structures and mineral chemistry of hydrated ferric sulfates. IV. The crystal structure of quenstedtite. American Mineralogist, 59 582–586.

Visser, J.W. (1969) A fully automatic program for finding the unit cell from powder data. Journal of Applied Crystallography, 2, 89–95.

Manuscript received May 7, 2004
Manuscript accepted August 6, 2004
Manuscript handled by Peter Burns